Electronic Supplementary Material (ESI) for Soft Matter

Supporting Information for

Tunable pH and Temperature Response of Weak Polyelectrolyte Brushes: Role of Hydrogen Bonding and Monomer Hydrophobicity

Yiming Lu, Aliaksandr Zhuk, Li Xu, Xing Liang, Eugenia Kharlampieva and Svetlana Sukhishvili

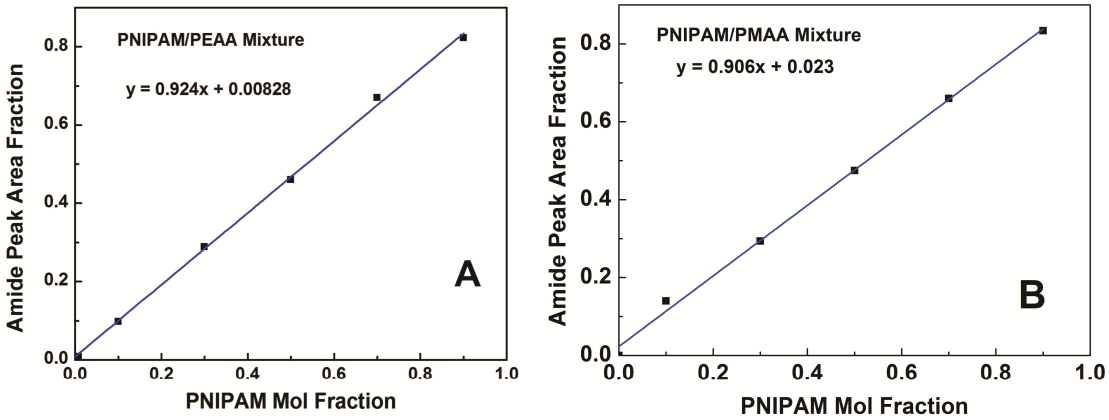

Fig. S1. A calibration curve obtained with mixtures of A) PEAA and PNIPAM or B) PMAA and PNIPAM of various compositions used for conversion of FTIR absorbances to molar compositions of P(aAA-*co*-NIPAM) copolymers.

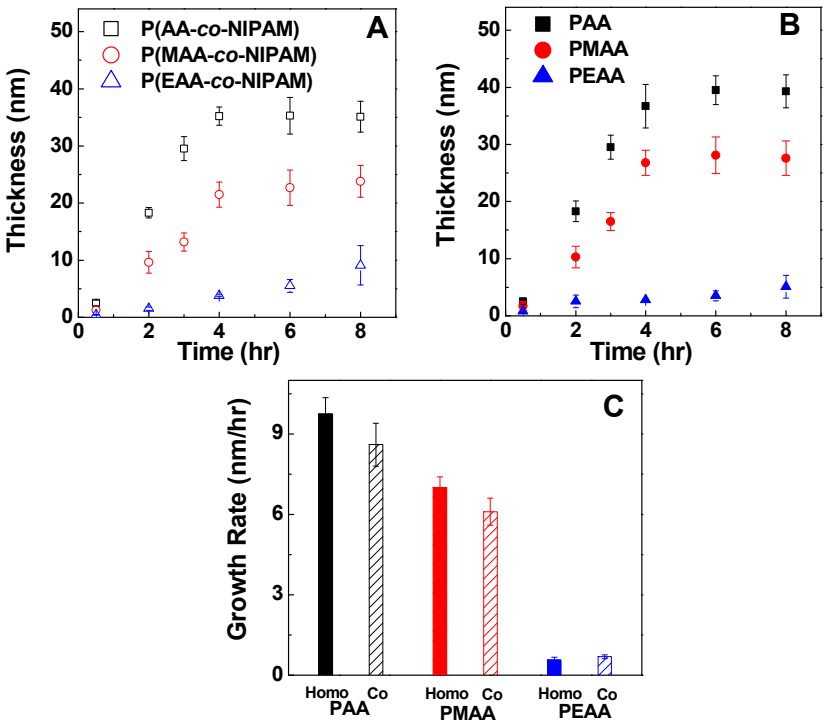

Fig. S2. Kinetics of brush growth for 7:3 P(aAA-co-NIPAM) copolymer and PaAA homopolymer brushes (A and B, respectively) as measured by ellipsometry. Each data point is an averaged over three points. C) Comparison of growth rates for PaAA homopolymers (solid bars) and P(aAA-co-NIPAM) copolymer brushes (patterned bars).

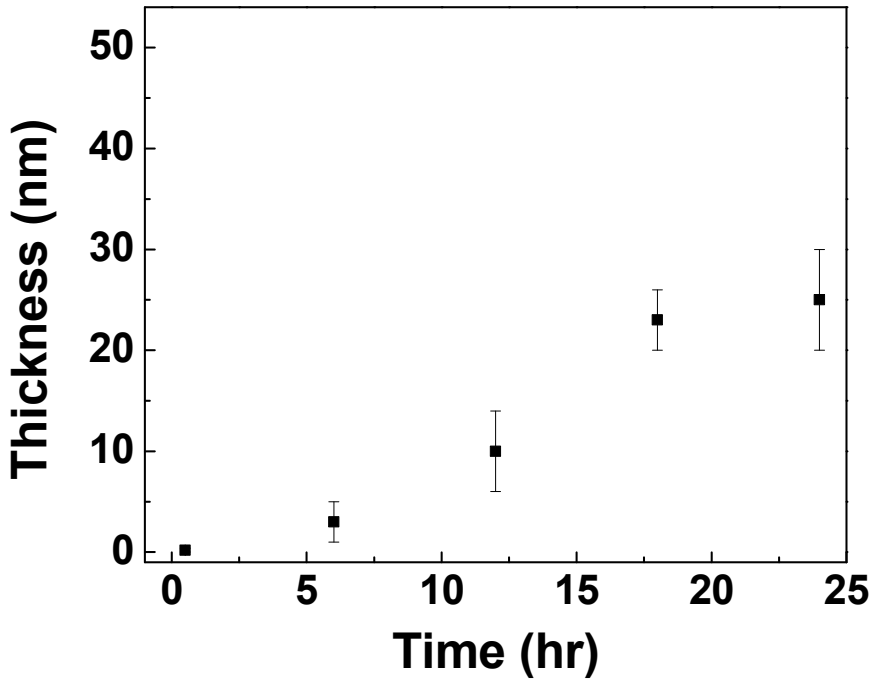

Fig. S3. Kinetics of brush growth for PNIPAM homopolymer brush.

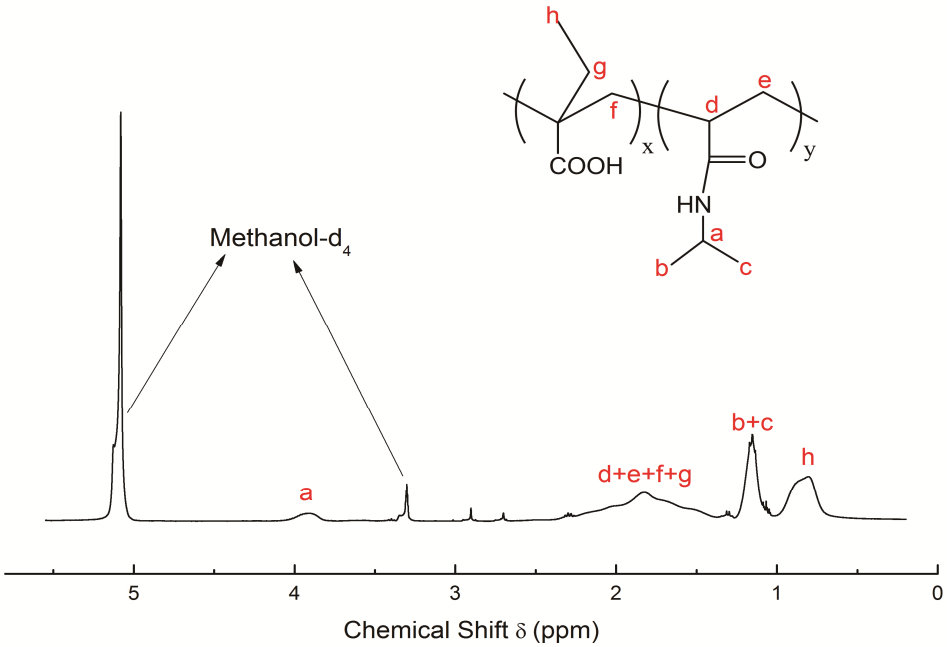

Fig. S4. Representative ^{1}H NMR spectrum of P(EAA-*co*-NIPAM) from solution polymerization. Solvent (methanol-d_4) peaks with chemical shifts at 4.9 ppm and 3.29 ppm are shown by arrows.

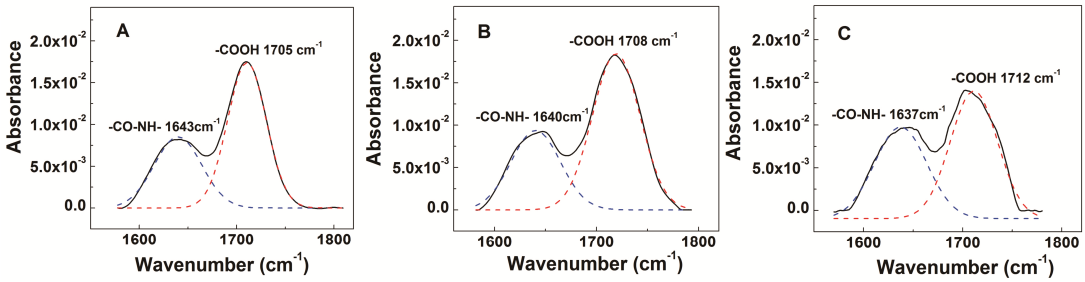

Fig. S5. FTIR transmission measurements of P(AA-*co*-NIPAM) (A), P(MAA-*co*-NIPAM) (B) and P(EAA-*co*-NIPAM) (C) brushes synthesized on undoped silicon wafers. Comparison of copolymer compositions included within brush or synthesized in solution using the same RAFT procedure and the same 7:3 acid:NIPAM molar feed ratio is illustrated in Table 2. Fractions of 2-alkylacrylic acid were determined using calibration curves shown in Fig. S1. In the cases of P(AA-*co*-NIPAM) and P(MAA-*co*-NIPAM) brushes (thicknesses 34.8nm and 35.5nm, respectively), measurements were performed with single silicon wafers. In the case of thinner P(EAA-*co*-NIPAM) brushes (thickness ~10nm), spectra were collected with a stack of three brush-modified wafers.

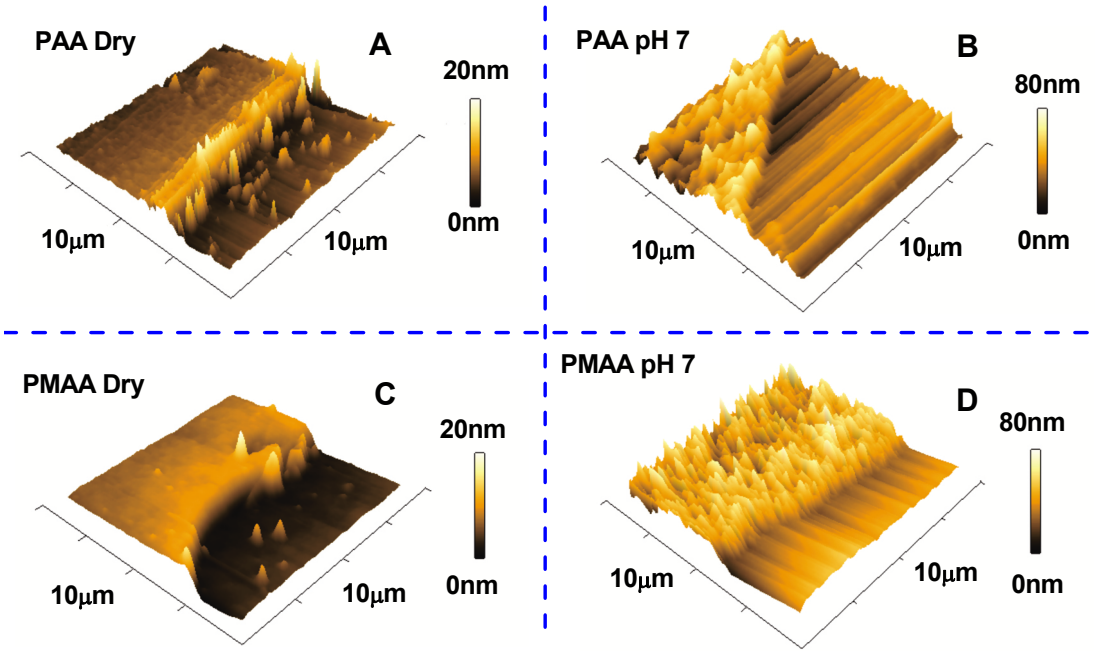

Fig. S6. AFM measurement of dry (A,C) and wet (B,D) PAA and PMAA homopolymer brushes, showing brush swelling ratios 3.5~4 times. Dry thickness of PAA and PMAA brushes was ~12 nm and ~ 15 nm, respectively.

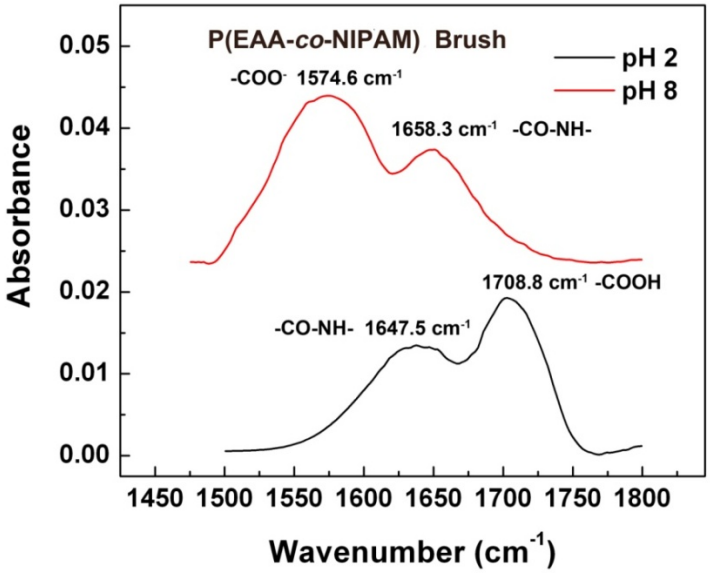

Fig. S7 FTIR spectra of P(EAA-*co*-NIPAM) copolymer brush exposed to pH 2 or pH 8 prior to measurements in a dry state (brush thickness ~ 10 nm). The absence of 1705 cm^{-1} band with wafers pre-exposed to pH 8 indicates complete ionization of carboxylic groups. FTIR spectra were collected with stacks of three identical brush-modified undoped wafers.

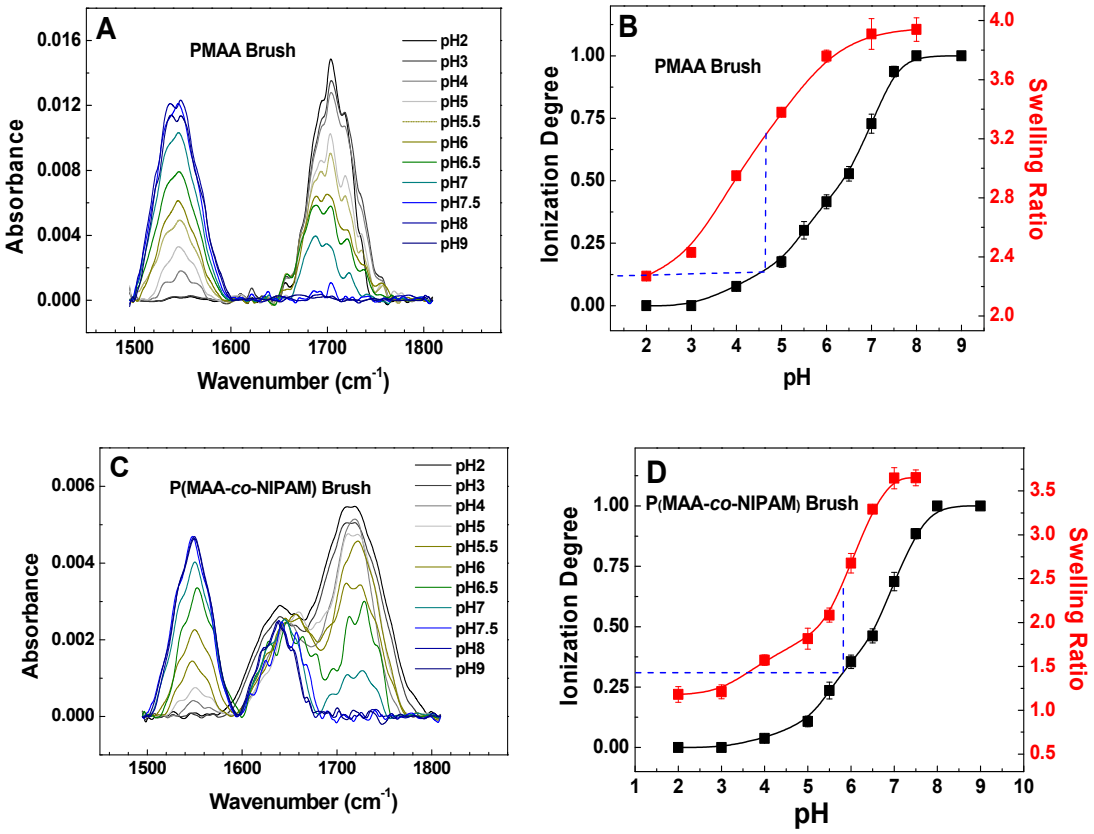

Fig. S8 FTIR spectra (A, C), calculated ionization degrees (α), and ellipsometric swelling ratios (B, D) for PMAA and P(MAA-*co*-NIPAM) brushes at 25°C. Blue dashed lines indicate pH values (pH 4.8 for PMAA and pH 5.8 for P(MAA-*co*-NIPAM) of half-swollen brushes, which correspond to α=0.125 for PMAA, and to α=0.25 for P(MAA-*co*-NIPAM) brush.

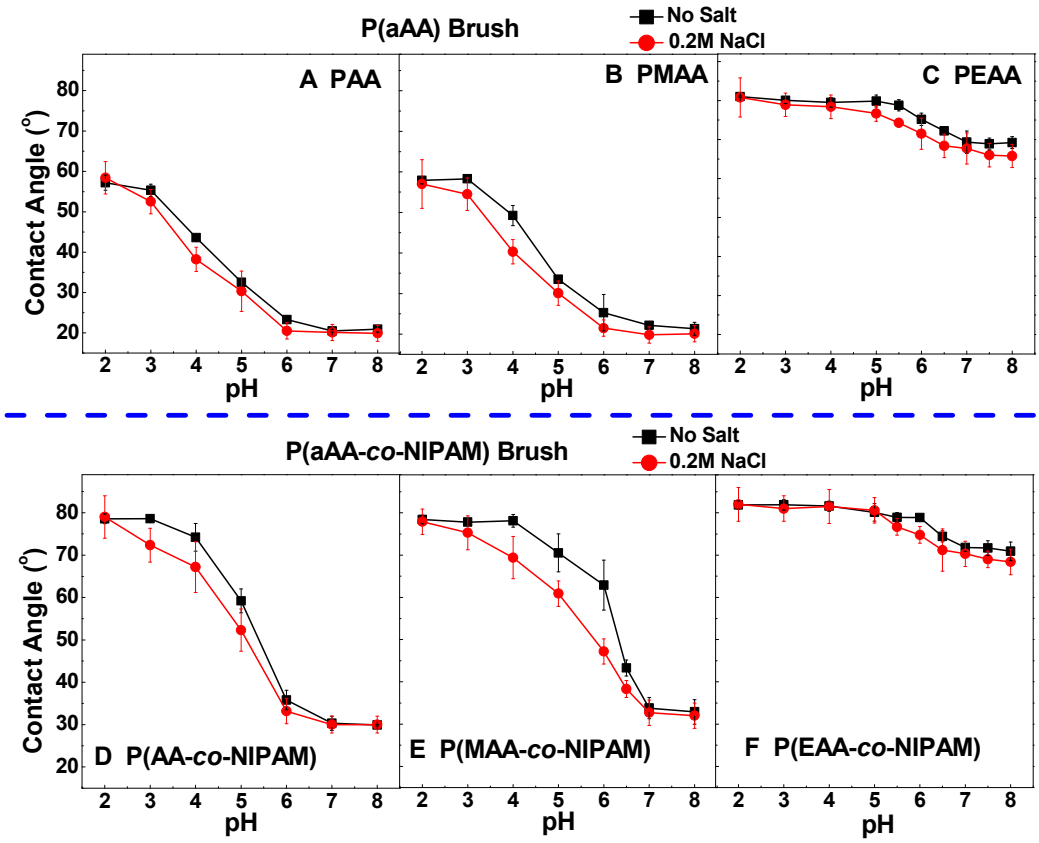

Fig. S9 Contact angles of P(aAA) homopolymer and P(aAA-*co*-NIPAM) copolymer brushes as a function of pH measured with 0.01 buffer solutions with and without 0.2M NaCl.

Table S1. Grafting densities for homo- and copolymers calculated based on GPC data of polymer solutions and ellipsometric thicknesses of corresponding brushes.

Polymer	Homopolymer		
	PAA	PMAA	PEAA
M_n (g/mol)	91,900	78,100	84,500
PDI	1.12	1.16	1.56
Thickness (nm)	35	28	6.5
Grafting Density (σ, chain/nm^2)	~ 0.27	~ 0.26	~ 0.09
Polymer	Copolymer (aAA:NIPAM = 7:3)		
	P(AA-*co*-NIPAM)	P(MAA- *co*-NIPAM)	P(EAA- *co*-NIPAM)
M_n (g/mol)	76,800	85,600	79,400
PDI	1.17	1.18	1.24
Thickness (nm)	32	25	10.3
Grafting Density (σ, chain/nm^2)	~ 0.24	~ 0.21	~ 0.1